Spring 2021

Quantifying Confinement of Chain Dynamics for Chains Tethered to Self-Assembling Crystalline Nanodomains Using Neutron Spin Echo Spectroscopy

Logan Benninghoff
ldb70@zips.uakron.edu

Quantifying Confinement of Chain Dynamics for Chains Tethered to Self-Assembling Crystalline Nanodomains Using Neutron Spin Echo Spectroscopy

An Honors Thesis

Presented to

The Faculty at the University of Akron

In Partial Fulfillment

Of the Requirements for the

Bachelor of Science Degree with Honors

Logan Benninghoff

April 2021

Quantifying Confinement of Chain Dynamics for Chains Tethered to Self-Assembling Crystalline Nanodomains Using Neutron Spin Echo Spectroscopy

Executive Summary

Tethering polymer chains to the surface of a nanodomain within a polymer nanocomposite with sufficiently high tethering density can lead to the formation of a polymer brush. A polymer brush is a collection of neighboring chains stretched from their preferred conformations by virtue of the large tethering density. A nanocomposite was created from side chain grafted polyisobutylene (PIB) backbones by the self-assembling of the side chains into crystalline nanodomains. The chemical structure of the PIB graft block copolymer molecule can be designed to alter the degree of chain stretching within the polymer brush at the surface of the nanodomain in order to obtain desirable macroscopic properties[1]. Our expectation was that the crowding of the stretched chains within a polymer brush will restrict their motion, leading to the chains in the polymer brush showing dynamics different from unstretched matrix chains. We investigated the polymer chain dynamics of three variations of this novel nanocomposite. Within these nanocomposites, the polymer chains are able to tether to multiple distinct nanodomains. We call this connecting between nanodomains "bridging". The effects of chain crowding at the nanodomain surface and bridging between nanodomains on the dynamics of the polymer chains were studied here.

We considered samples of three polyisobutylene (PIB) graft copolymer molecules reinforced by crystalline nanodomains formed by self-assembly of the graft side chains. Schematics of the molecular structures of 68, 77, and 94 are shown in Figure 1. Small angle neutron scattering (SANS) was used to determine the morphology of the nanocomposite and neutron spin echo spectroscopy (NSE) was used to quantify the samples' chain dynamics. The samples were swollen with deuterated cyclohexane (dCH) to create contrast for the scattering and to move the chain dynamics into a range accessible with NSE. Sample 68 had the highest volumetric swelling ratio, while sample 77 had the lowest volumetric swelling ratio.
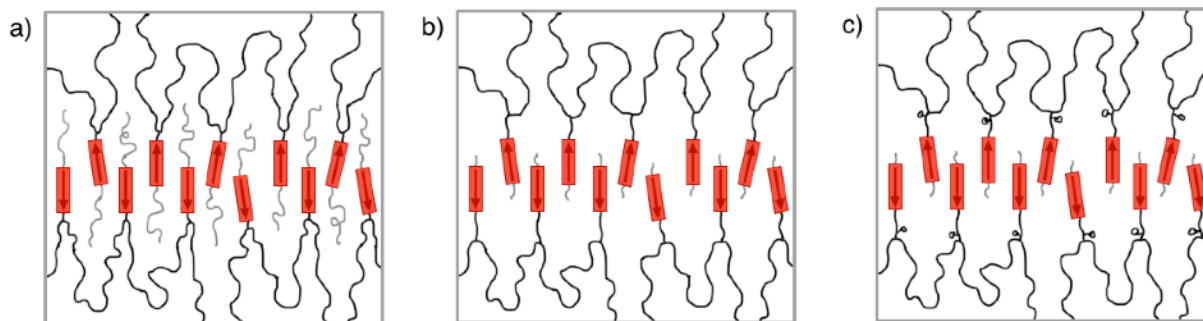
Figure 1. Schematics of a) 68, b) 94, and c) 77. The PIB backbone chains and the spacer chain between the backbone and β-alanine oligomers are shown in black, and the aliphatic tail is shown in gray. The β-alanine oligomers which self-assemble into nanodomains are shown in red, with an arrow pointing towards the spacer chain and way from the aliphatic tail. Note that there is a benzene ring present on the spacer chain for 77.

Plots of intensity vs. scattering vector, Q, obtained from SANS measurements were fit using a core-shell parallelepiped model[2] within the Q range of interest. The parameter fits to the SANS data showed that the height of a region of chains not immediately adjacent to the crystal surface, but still stretched, was 70.2 ± 0.3 Å for sample 68 and 94 ± 1 Å for samples 77 and 94. The parameter fits also showed that sample 68 forms the smallest nanodomains, with a mean length of 140 ± 20 Å in the hydrogen bonding direction of the crystal. The SANS data indicates that sample 77 forms smaller domains than does 94, but the lengths of those two samples' nanodomains were too large to be resolved precisely. Their crystal lengths were at least 3000 Å in the hydrogen bonding direction. The polymer chains at the crystal surface of sample 68 were the most densely crowded. This is because the spacer chain that connects the nanodomain surface and PIB backbone is shorter, so the spacer chain branches out into two backbone portions closer to the surface. This is consistent with sample 68 forming the smallest nanodomains, because the entropic penalty for nanodomain growth is higher due to increased crowding near the surface. The spacer chains of samples 77 and 94 are longer than those of 68. Thus, there was less crowding near the crystal surface and samples 77 and 94 formed larger domains. Sample 77 forms smaller domains than does 94 because there is a benzene ring attached to the spacer chain of 77 which increases crowding.

Plots of normalized intermediate scattering function, $I(Q,t)/I(Q,0)$, vs. Fourier time for 68, 77, and 94 were obtained from NSE measurements done at the Center for High Resolution Neutron Scattering (CHRNS) at National Institute of Standards and Technology. The $I(Q,t)/I(Q,0)$ data were fit using a Kohlrausch-Williams-Watts (KWW)[3,4] stretched exponential function with the form,

$$I(Q,t)/I(Q,0) = I_o \exp(-(t/\gamma)^\beta), \qquad (1)$$

where β, the stretching parameter, can take on values between 0 and 1, and γ is the relaxation time. The resulting variation of relaxation time with Q was compared to that expected for the Zimm model of polymer chain dynamics. For a system that displays Zimm-like[5,6] dynamics we expected the relaxation time γ to scale with Q^{-3}, so we plotted $I(Q,t)/I(Q,0)$ vs. Fourier time scaled by Q^3. Intermediate scattering functions that show a Q^{-3} dependence overlap on these scaled plots. Significant overlap of these curves was seen for all three samples, with the curve for sample 68 having the least overlap, and therefore the broadest region of Q where dynamics deviating from Zimm-like behavior were observed. Sample 77 had the most overlap, giving it the most narrow region of Q over which dynamics deviating from Zimm-like behavior were observed. To determine the parameter values of the curves that show Zimm-like behavior, we modified the stretched exponential function by substituting $\tau*Q^{-3}$ for γ,

$$I(Q,t)/I(Q,0) = A \exp(-(t/(\tau*Q^{-3}))^\beta), \qquad (2)$$

where τ is the characteristic relaxation time for the sample in the Q region containing chains with Zimm-like behavior. The portions of the data curves that deviated from the master curve on the scaling plot were masked, then the master curve was fit using the modified stretched exponential function. The Q regions where Zimm-like behavior were observed for the chains corresponded to length scales at which the dynamics of the unstretched chains in the matrix dominated. Therefore, the parameter fits from the modified stretched exponential described the Zimm-like behavior of the matrix chains.

To quantify the dynamics of the stretched chains surrounding a nanodomain, we modified our stretched exponential again, fitting the intermediate scattering functions with a function of the form[7],

$$I(Q,t)/I(Q,0) = I_o(A \exp(-(t/(\tau Q^{-3}))^\beta) + (1-A)), \qquad (3)$$

where the first term gives the contribution from chains showing Zimm-like behavior as in (2), using τ and β values from the fits of the I(Q,t)/I(Q,0) vs. scaled Fourier time plots. The first term containing A reflects the relative contribution of Zimm behavior. The (1-A) term accounts for the contribution from chains with non-Zimm dynamics with relaxation times slower than 100 ns, which was the largest timescale measured in the experiment. The new function provided fits with errors comparable to those for the KWW stretched exponential function fits, but using only two parameters instead of three. We then plotted A vs. Q to compare the size of the regions of Q where we saw non-Zimm behavior for each sample, as shown in Figure 2.
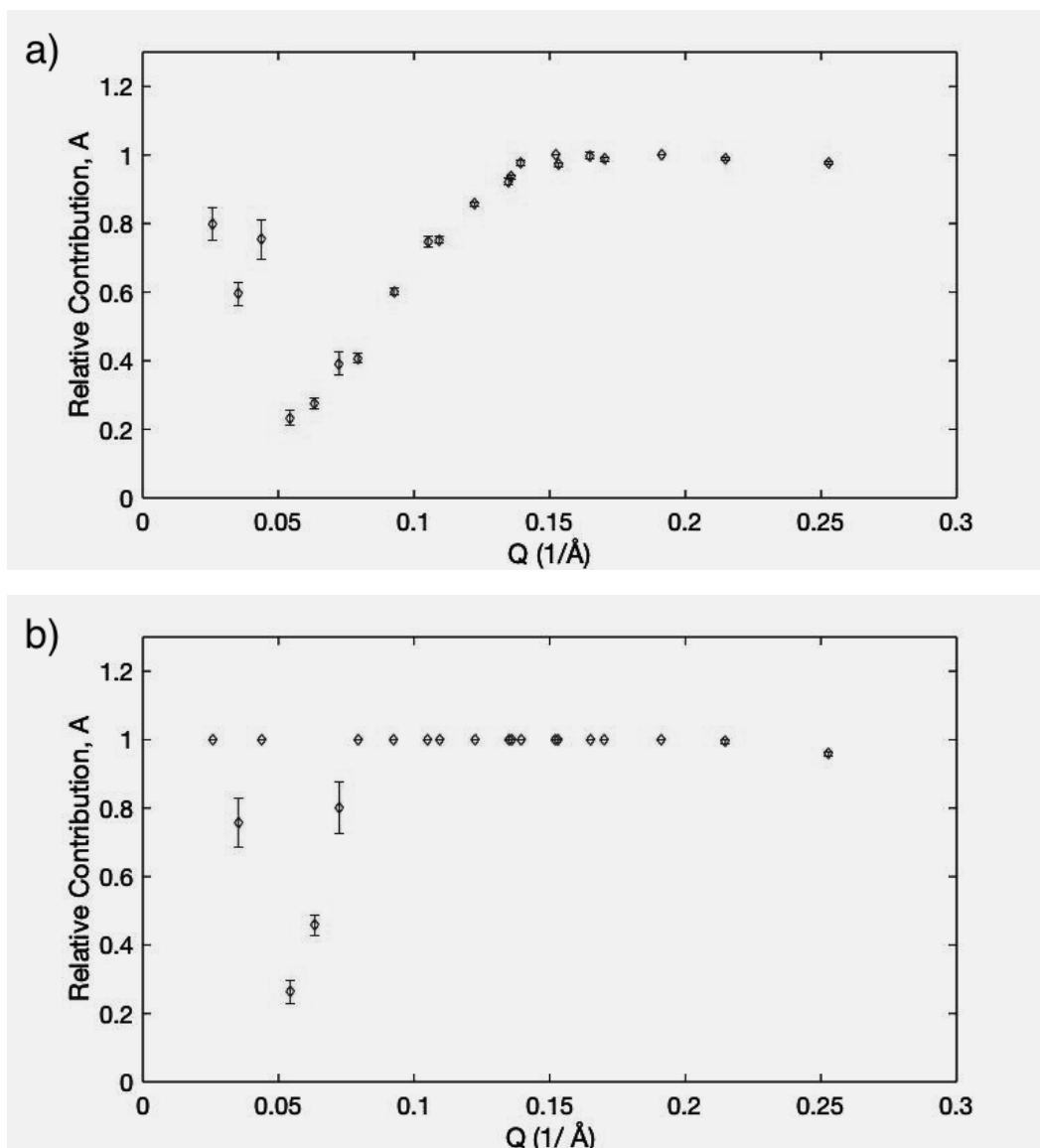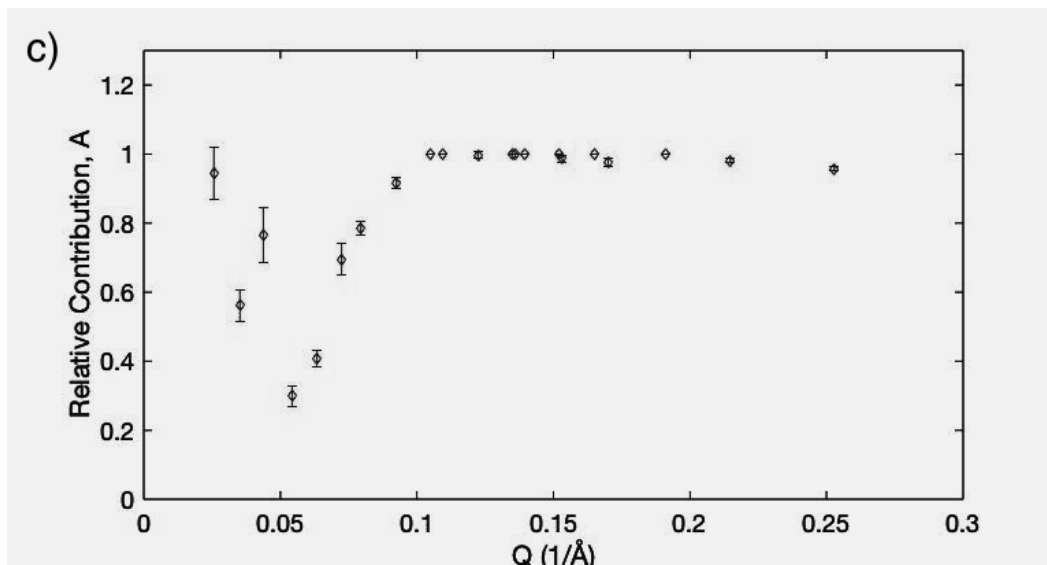
Figure 2. Plots of the relative contribution of Zimm dynamics (parameter A) for a) 68, b) 77, and c) 94 as a function of Q. Values of A equal to 1 correspond to polymer chains showing entirely Zimm behavior. Values of A equal to 0 would indicate no relaxation at all on the time sales probed (entirely non-Zimm behavior). We see that the samples never exhibit entirely non-Zimm behavior, with a minimum A value around 0.2 for all three samples. Sample 68 shows chain dynamics with non-Zimm behavior over the broadest range of Q. Sample 77 shows chain dynamics with non-Zimm behavior over the narrowest range of Q.

The presence of the (1-A) term in the normalized intermediate scattering function which corresponds to chains not relaxing on the time scales probed is consistent with the notion that chain confinement occurs due to the crowding of chains at the crystal surface. The approximation $L = 2\pi/Q$ was used to determine the length scales over which confined dynamics are observed. Sample 68 showed some influence of confinement at the highest Q value, around 0.15 Å^{-1}, which corresponds to a length scale of ca. 45 Å. On length scales smaller than 45 Å we saw Zimm-like behavior. We know from the SANS fit that the region of stretched chains not immediately adjacent to the crystal surface, but still stretched, is ca. 70 Å for sample 68. Within the SANS model the more complicated behavior of this region is approximated by assuming a uniform behavior averaged across the region. Thus, we would expect to see the strongest effects of confinement on a length scale lower than 70 Å. Seeing confined dynamics at a length scale ca.

6

45 Å and above for 68 then suggests that we are seeing the effects of confinement within this region of stretched chains. The largest contribution of confined dynamics for all three samples was seen at $Q = 0.055$ Å^{-1} which corresponds to a length scale of ca. 110 Å. The mean distances between nanodomains for all three samples lie between 100 Å and 130 Å. Since we see the largest confined dynamics on a length scale corresponding to the distances between nanodomains, we hypothesize that this confinement is due to bridging between nanodomains.

Acknowledgements

References

(1) Srivastava, A.; Zhao, Y.; Meyerhofer, J.; Jia, L.; Foster, M. D. Design of Interfacial Crowding for Elastomeric Reinforcement with Nanocrystals. *ACS Appl. Mat. & Interf.* **2021**, *13*, 10349-10358.

(2) Mittelbach, P.; Porod, G. Zur Röntgenkleinwinkelstreuung Verdünnter Kolloider Systeme. Die Berechnung der Streukurven von Parallelepipeden. *Acta Phys. Austriaca* **1961**, *14*, 185–211.

(3) Kohlrausch, F. Ueber die elastische Nachwirkung bei der Torsion. *Ann. Phys.* **1863**, *195*, 337-368.

(4) Williams, G.; Watts, D. C. Non-symmetrical dielectric relaxation behaviour arising from a simple empirical decay function. *Trans. Faraday Soc.* **1970**, *66*, 80-85.

(5) Richter, D.; Kruteva, M.; Polymer dynamics under confinement. *Soft Matter* **2019** *15*, 7316-7349.

(6) Zimm, B. H.; Kilb, R. W. Dynamics of Branched Polymer Molecules in Dilute Solution. *J. Polym. Sci.* **1959**, *37* (131), 19-42.

(7) Richter, D.; Monkenbusch, M.; Arbe, A.; Colmenero J. *Neutron Spin Echo in Polymer Systems*. Advances in Polymer Science. *174*, Springer, Berlin, Heidelberg, 2005. And references therein.

(8) Azuah, R.T.; Kneller, L.R.; Qiu, Y.; Tregenna-Piggott, P.L.W.; Brown, C.M.; Copley, J.R.D.; Dimeo, R.M. DAVE: A comprehensive software suite for the reduction, visualization, and analysis of low energy neutron spectroscopic data. *J. Res. Natl. Inst. Stan. Technol.* **2009**, *114*, 341.